

Perspective of a hydrographic LIDAR in space: Specifications and results of a simulation

Rainer Reuter and Oliver Zielinski
Carl von Ossietzky University of Oldenburg
Physics Department, D-26111 Oldenburg, Germany*

ABSTRACT

Long-term surveillance of coastal zones like the German Bight with airborne laser fluorosensors have shown the capability of active remote sensing to investigate various oceanic parameters, such as dissolved organic matter (gelbstoff) or chlorophyll in algae.

Recently the feasibility of a spaceborne laser fluorosensor for large-scale monitoring of water-column parameters has met increasing interest. Complementary to passive remote sensing instruments, like SeaWiifs or OCTS, active remote sensing promises to provide a powerful tool for detection of substances which are otherwise hardly detectable, using inherent molecular fluorescence at specific wavelengths.

The feasibility of such measurements using platforms at altitudes of up to 800 km is studied. This would allow the instrument to be operated as an attachment to atmospheric lidars.

A simulation of radiative transfer in a cloudless and horizontally stratified atmosphere is presented, with particular emphasis on wavelengths which are relevant for hydrographic measurements. Results of this simulation are presented, especially the geometrical aspects of radiative transfer through the atmosphere, optimisation of lidar parameters and effects of dispersion.

Keywords: hydrographic lidar, laser fluorosensor, ocean monitoring, radiative transfer, gelbstoff, biooptics

1 INTRODUCTION

Ocean monitoring has met with increasing interest in pollution control, as well as in global survey of biological and hydrological components like chlorophyll in algae or dissolved organic matter (denoted as gelbstoff). Especially in the context of global carbon flux estimations and climatological modelling efforts, the ocean as a carbon sink and the related phytoplankton distribution have come into focus. Passive remote sensing instruments like SeaWiifs or OCTS try to estimate biomass from ocean color data [6,17]. Other sensors provide additional hydrographic information like e.g. sea surface temperature (SST) and sea surface elevation from which information on currents and upwelling processes can be deduced.

However, certain oceanic parameters are difficult to detect with passive remote sensing instruments. Dissolved organic matter DOM, mostly called gelbstoff or yellow substance, is one example since it is present in open ocean (case 1) waters at too low concentrations to affect ocean color. Its measurement over large scales would be of high interest since it plays an important role in the global carbon cycle [3]. Using the inherent molecular fluorescence of these substances allows their measurement with active laser fluorosensors. Theory

* For further information see WWW: <http://www.physik.uni-oldenburg.de/Docs/las/> or send Email to r.reuter@las.physik.uni-oldenburg.de or oliver@las.physik.uni-oldenburg.de

and application of these instruments have been extensively described in the literature [4,5,13,15,16]. A brief description of signals from natural organic compounds of seawater, like gelbstoff and phytoplankton chlorophyll *a* will be given in the following section. Ocean monitoring on basin-wide global scales is difficult with airborne instruments, especially over long time periods. Therefore, the feasibility of active lidar measurements from altitudes of up to 800 km has met with increasing interest, since they would allow large-scale and continuous surveys.

2 FLUORESCENCE MEASUREMENTS OF BIOOPTICAL PARAMETERS

The optical characteristics of organic substances include wavelength specific absorption as well as fluorescence. The list of detectable components includes gelbstoff, chlorophyll *a*, and other phytoplankton pigments like phycoerythrin, fucoxanthin and fucocyanin [2,14]. In this paper only gelbstoff and chlorophyll *a* are considered. Fig. 1 shows a typical emission spectrum of coastal (case 2) seawater containing gelbstoff and algae, taken with a laboratory instrument ($\lambda_{ex} = 308$ nm). One finds:

- The water Raman peak at 344 nm resulting from the inelastic scattering of light at the H₂O-molecules (Stokes shift of water ~ 3400 1/cm).
- The spectrally broad fluorescence of yellow substances with a characteristic maximum at 420 nm. Absorption of gelbstoff is antiproportional to the wavelength and thus leads to high fluorescence intensities with UV excitation.
- Chlorophyll *a* fluorescence from photosystem II about 680 nm.

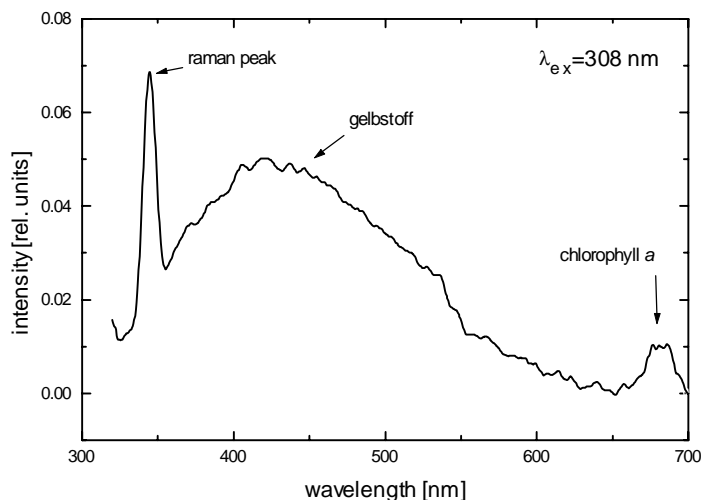


Fig. 1. Laboratory fluorescence spectrum of a seawater sample containing algae and yellow substance with an excitation wavelength of 308 nm. The sample has been taken in the German Bight at 54°15'N, 07°44'E on 05/05/1994.

Table 1 compares a number of parameters for four selected wavelengths. The Raman efficiency was calculated from the Raman scattering coefficient of water, showing the typical λ^4 wavelength dependence like Rayleigh scattering [7]. Gelbstoff and chlorophyll fluorescence efficiency is derived from laboratory experiments and depends on the type of water and class of algae. Case 2 water samples from the German Bight were used, containing terrestrial compounds of humic substances. The optimal fluorescence efficiency for chlorophyll *a* is at an excitation wavelength of 420 nm. Chlorophyll *a* shows an absorption gap from 470 nm to 660 nm which results in the low efficiency of the 532 nm excitation. However, depending on the class of algae there are different absorption characteristics due to a variety of pigments involved (e.g. carotene). Thus further investigations are planned for classification of spectral signatures from these substances.

Table 1: Comparison of excitation wavelength

Excitation wavelength [nm]	270	308	355	532
Raman peak wavelength [nm]	297	344	404	650
Raman efficiency [rel. units]	1.00	0.59	0.33	0.07
Gelbstoff fluorescence efficiency [rel. units]	1.00	0.53	0.31	--
Chl. fluorescence efficiency [rel. units]	0.40	0.72	0.76	0.06

3 MEASUREMENTS FROM SPACE

While airborne fluorosensing of maritime pollution is carried out routinely in coastal zones, this method is not yet available for measurements in larger oceanic regions. However, global monitoring programmes like e.g. the Earth Observing System EOS call for a long-term and large-scale investigation of oceanographic processes in the world oceans. Some of the parameters to be measured in these programmes can be assessed with hydrographic lidar in space. It will be the object of this chapter to present a simulation of such an instrument, to show up solutions of some specific problems and outline the potential of a combined hydrographic/atmospheric lidar in space.

3.1 Radiative transfer in the atmosphere

Possible space platforms for a hydrographic lidar include the Space Shuttle at 300 km, space stations like MIR at 400 km and satellites on lower earth orbits at up to 800 km above sea level. It is common to measurements from these altitudes that the laser beam and the detected fluorescence of a lidar are subject to atmospheric influences that weaken and deflect the signal. In addition there exists a solar induced background signal, strongly depending on actual weather conditions and the angle between sun and detector. The signal-to-background ratio is essential for information retrieval and it will be important to improve this ratio by technical progress. Possible sources of atmospheric influences for the optical information in the visible and near ultra-violet region are:

- Rayleigh scattering, with the typical λ^{-4} dependence
- Absorption by ozone (O_3) - especially below 320 nm this factor is considerably high
- Attenuation by tropospheric and stratospheric aerosols

In addition to these well-known effects [9, 10], there are two factors that should be examined for a complete description. A hydrographic lidar in space will change its position during the time of light propagation in the atmosphere, thus a small angular correction will be necessary¹. On the other hand, a beam of light started under a laser-zenith-angle $\neq 0^\circ$ is manipulated by the variable refraction index of air. This results in a so-called *slant path* and by modeling the radiative transfer in the atmosphere it will be possible to calculate the exact deviation and attenuation of an optical signal.

¹ For a flight altitude of 300 km the light takes approximately 2 ms for its way down to the sea surface and back to the detector. During this time the platform moves ~ 15.5 m. Consequently the centres of the laser illuminated region and the detector field of view also show up a distance of ~ 15.5 m. Assuming circular patterns and a 0.6 mrad divergence for both components this would lead to an overlap of only 89% of the possible maximum overlap area. A small angular correction of -0.0029° at the detector for a nadir-looking laser would compensate this movement and allow for a 100% overlap, independent of the chosen divergence.

3.2 Simulation of a hydrographic lidar-in-space

In this simulation a cloudless and horizontally stratified atmosphere is taken into consideration. For the purpose of testing, the US Standard Atmosphere of 1962 with additional information on ozone and aerosols is applied [10]. The refractive index $n(z)$ at an altitude z depending on the temperature $T(z)$, the partial pressure of air $p(z)$, the partial pressure of water vapor $p_{\text{H}_2\text{O}}(z)$, and the wavelength λ are calculated using the equation by McClatchey and Selby [11]:

$$(n(z) - 1) 10^6 = \left(77.46 + \frac{0.459 \mu\text{m}^2}{\lambda^2} \right) - \frac{p(z) \text{ K}}{T(z) \text{ hPa}} - \frac{p_{\text{H}_2\text{O}}(z)}{1013 \text{ hPa}} \left(43.49 - \frac{0.347 \mu\text{m}^2}{\lambda^2} \right). \quad (1)$$

For the slant path calculation we solve Fermats variation principle, stating that light always takes the shortest optical path, via the Euler-Lagrange differential equation. Implementing this solution in an integration over the altitude z the deviation x at height z_2 of a lightbeam of wavelength λ starting at z_1 at an angle $\Theta(z_1)$ can be calculated by

$$x(z_2) = x(z_1) + \int_{z_1}^{z_2} \frac{n(z_1)}{n(z)} \sin \Theta(z_1) \left(1 - \left(\frac{n(z_1)}{n(z)} \right)^2 \sin^2 \Theta(z_1) \right)^{-1/2} dz, \quad (2)$$

with $n(z)=n(T, p, p_{\text{H}_2\text{O}}, \lambda)$ being the refractive index of air following equation (1). It was mentioned before that the movement of the platform during the time of light propagation calls for a small angular correction e.g. at the detector. In the first approximation one can show that a detector under an angle of

$$\sin \Theta_{\text{det}} = \left(x_{\text{det}} - x_{\text{probe}} \right) / \int_{z_{\text{probe}}}^{z_{\text{laser}}} \frac{n(z_{\text{probe}})}{n(z)} dz, \quad (3)$$

will correct the platform movement, if x_{probe} is the centre of the laser illuminated area calculated via Eq. (2) and x_{det} is approximated by

$$x_{\text{det}} \approx 2 t v_{\text{sat}}, \quad (4)$$

with t being the time the laser pulse takes from the platform to the sea surface.

Calculating the deviation of a lightbeam following Eq. (3) for different wavelengths λ it is possible to estimate the effect of dispersion at a given laser-zenith-angle Θ_{laser} . Fig. 2 shows the difference of these deviations x_{probe} at 685 and 308 nm. One can see that the wavelength dependence of the refractive index can be practically neglected for $\Theta_{\text{laser}} < 60^\circ$. Furthermore, it is possible to calculate complete scan patterns of a possible hydrographic lidar, using the given equations, for reasons of optimization and illustration. Fig. 3 shows such a scan pattern for an altitude of 300 km covering the German Bight.

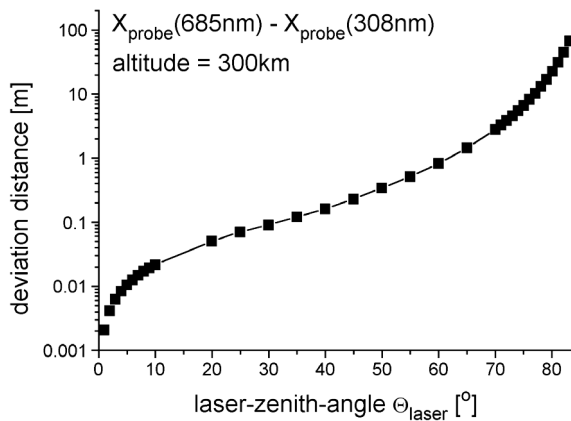


Fig. 2. Effect of dispersion for a laser beam starting at 300 km altitude under a variable laser-zenith-angle Θ_{laser} measured via the deviation distance for two wavelengths.

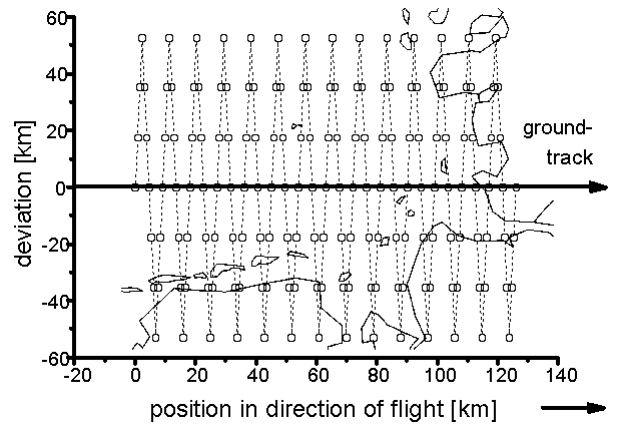


Fig. 3. Example of a scan pattern (altitude 300 km, $\lambda=355$ nm, average pulse repetition rate 10 Hz, max. scan angle 10°). A part of the German Bight was projected into the plot.

3.3 Layout of a spaceborne lidar

Utilizing the model in section 3.2 it is possible to simulate a hydrographic lidar in space under the given limitations of the approach (see Fig. 4 for illustration). That includes possible scan configurations as well as footprint diameters for different beam divergences. Flight altitudes were chosen with respect to standard space carrier, like the Space Shuttle, the Mir station or satellites on lower earth orbit. Required laser energies can be calculated by the lidar equation and have to satisfy eye safety regulations (see Bartsch et al. [1]).

An important task is the selection of the excitation wavelength for oceanic measurements. A possible laser source is a frequency tripled Nd:YAG-laser since its 355 nm emission wavelength is in the absorption gap of ozone in the spectral region between 350 and 450 nm. Following section 2 this excitation is capable of inducing gelbstoff and chlorophyll fluorescence. In addition, Matvienko et al. [8] proposed to apply the 1064 nm emission for simultaneous retrieval of atmospheric information. In fact the Nd:YAG-laser wavelength is well known from atmospheric missions like the Lidar In-Space Technology Experiment (LITE) [12]. A combined hydrographic/atmospheric lidar offers the possibility to combine oceanic measurements with actual atmospheric corrections, yielding quantitative concentrations of fluorescent matter in the surface layer of the ocean. Detection wavelengths are selected with respect to the measurable parameters and necessary baseline corrections. Table 3 summarizes some proposed features of a hydrographic lidar in space.

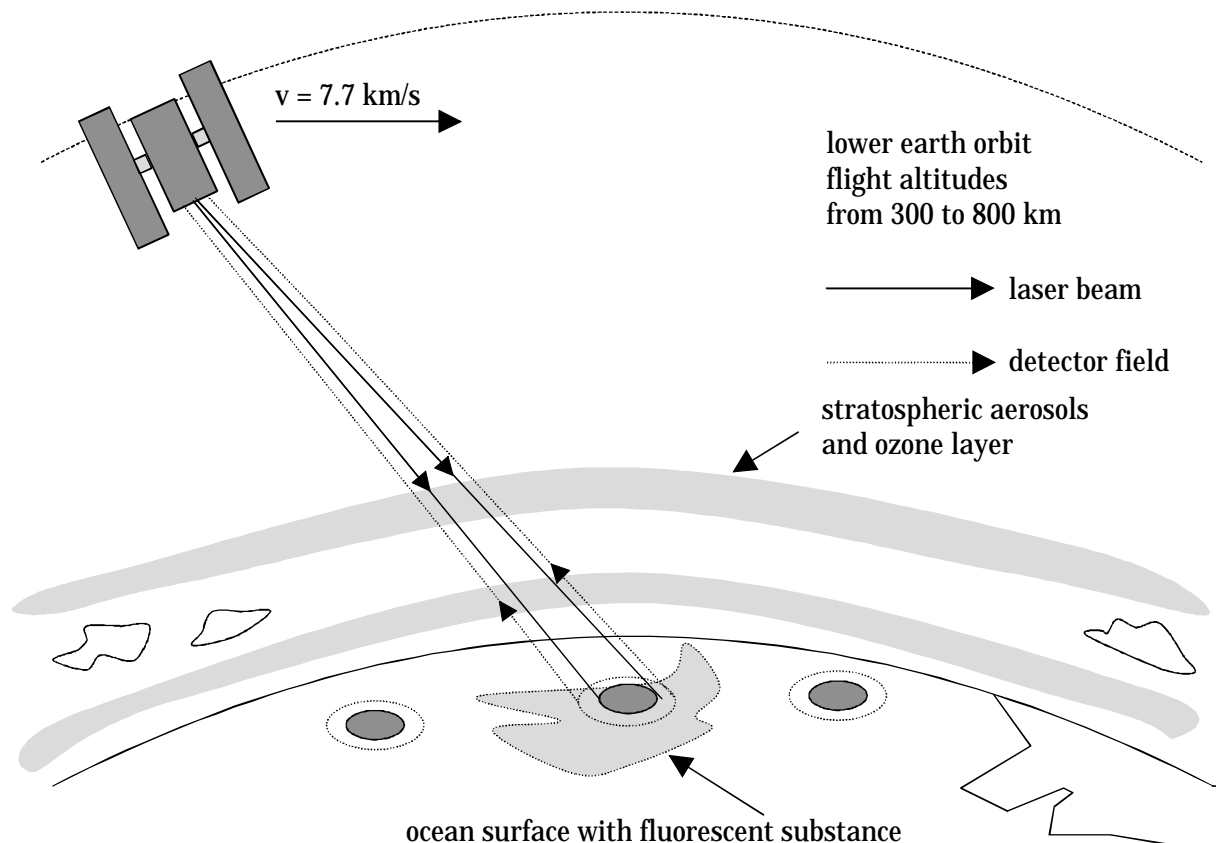


Fig. 4. Illustration of a hydrographic lidar in operation.

Table 3: Proposed layout of a hydrographic lidar in space

Operating properties			
flight altitude	300 km	or	800 km
speed of flight	7730 m/s	or	7800 m/s
Laser			
emission frequencies	Nd:YAG		
	1064 nm	and	355 nm
beam divergence	0.3 mrad		
pulse rep. rate	10 Hz		
Scanner			
	modified sine-pattern		
full scan angle	20° across-flight		
pixel-to-pixel distance	740 m		770 m
footprint diameter	90 m		240 m
Detector			
telescope	Cassegrain		
field of view	0.3 mrad		
channels	7 discrete, 355 - 380 - 404 - 430 - 620 - 685 - 1064 nm		

4 DISCUSSION

We have stated that a spaceborne hydrographic lidar offers the possibility of long-term and large-scale monitoring of biooptical components like yellow substance and chlorophyll in algae. To propose some design parameters for a possible instrument we have analysed the requirements for oceanic measurements, namely the selection of detection channels and the expected fluorescence efficiencies depending on the excitation wavelength.

The simulation of radiative transfer via a specific solution of Fermats principle enables the optimization of lidar angle configuration. We can also show that effects caused by dispersion in the atmosphere can be neglected at small laser-zenith-angles. For an improved correction of fluorescence signals a simultaneous measurement of atmospheric parameters by a combined hydrographic/atmospheric lidar or the use of an IR-backscatter signal (e.g. 1064 nm) is proposed. It is outlined that the frequency tripled Nd:YAG-laser (355 nm) provides an effective excitation wavelength for all discussed parameters and also matches atmospheric restraints like the strong ozone-absorption below 320 nm.

Future work in this project includes evaluation of different detection wavelengths, expansion of the simulation with respect to turbulence and earth curvature, and the development of algorithms for data correction using simultaneously measured atmospheric parameters.

REFERENCES

1. B. Bartsch, T. Braeske and R. Reuter, „Oceanic lidar: radiative transfer in the atmosphere at operating altitudes from 100 m to 100 km“, *Applied Optics* **32**, No. 33, 1993.
2. Determann, S., R. Reuter, P. Wagner and R. Willkomm, „Fluorescent matter in the eastern Atlantic Ocean Part 1: method of measurement and near-surface distribution“, *Deep-Sea Research* **41**, pp. 659-675, 1994.
3. H.W. Ducklow, C.A. Carlson, N.R. Bates, A.H. Knap and A.F. Michaels, „Dissolved organic carbon as a component of the biological pump in the North Atlantic Ocean“, *Phil. Trans. R. Soc. Lond. B* **348**, pp. 161-167, 1995
4. F.E. Hoge, R.E. Berry and R.N. Swift, „Active-passive airborne ocean color measurement. 1: Instrumentation“, *Applied Optics* **25**, pp. 39-47, 1986.
5. F.E. Hoge, R.N. Swift and J.K. Yungel, „Active-passive airborne ocean color measurement. 2: Applications“, *Applied Optics* **25**, pp. 48-57, 1986.
6. J. Marra, „Primary production in the North Atlantic: measurements, scaling, and optical determinants“, *Phil. Trans. R. Soc. Lond. B* **348**, pp. 153-160, 1995
7. B.R. Marshall and R.C. Smith, „Raman scattering and in-water ocean optical properties“, *Applied Optics* **29**, 1990.
8. G.G. Matvienko, G.P. Kokhanenko, M.M. Krekova, I.E. Penner and V.S. Shamanayev, „Representivity of the spaceborne lidar sounding of the upper sea layer“, *Lidar Techniques for Remote Sensing II*, SPIE Vol. 2581, 1995.
9. E.J. McCartney, „Optics of the Atmosphere - Scattering by Molecules and Particles“, *John Wiley & Sons*, 1976
10. R.A. McClatchey, R.W. Fenn, J.E.A. Selby, F.E. Volz and J.S. Garing, „Optical Properties of the Atmosphere (Third Edition)“, *AFCRL-72-0497*, *Envir. Res. Papers* No. 471, 1972.
11. R.A. McClatchey and J.E.A. Selby, „Atmospheric Transmittance from 0.25 to 28.5 μ m: Computer Code LOWTRAN 3“, *AFCRL-TR-75-0255*, *Envir. Res. Papers* No. 513, 1975.
12. M.P. McCormick, D.M. Winkler, E.V. Browell, J.A. Coakley, C.S. Gardner, R.M. Hoff, G.S. Kent, S.H. Melfi, R.T. Menzies, C.M.R. Platt, D.A. Randall and J.A. Reagan, „Scientific Investigations Planned for the Lidar In-Space Technology Experiment (LITE)“, *Bulletin of the American Meteorological Society* **74**, No. 2, 1993
13. R.M. Measures, „Laser Remote Sensing. Fundamentals and Applications“, *John Wiley & Sons*, 1984.
14. R. Reuter, D. Diebel and T. Hengstermann, „Oceanographic laser remote sensing: measurement of hydrographic parameters in the German Bight and in the Northern Adriatic Sea“, *International Journal of Remote Sensing* **14**, pp. 823-844, 1993.
15. R.Reuter, H.Wang, R. Willkomm, K. Loquay, T. Hengstermann and A. Braun, „A laser fluorosensor for maritime surveillance: Measurement of oil spills“, *EARSel Advances in Remote Sensing* **3**, pp. 152-169, 1995.
16. R. Reuter, R. Willkomm, O. Zielinski and W. Milchers, „Hydrographic Laser Fluorosensor: Status and Perspectives“, *Proc. of EuroGOOS*, to be published, 1997
17. T. Platt, S. Sathyendranath and A. Longhurst, „Remote sensing of primary production in the ocean: promise and fulfilment“, *Phil. Trans. R. Soc. Lond. B* **348**, pp. 191-202, 1995